Phytofabrication and characterization of silver nanoparticles and their enhanced antimicrobial activity

Preeti Sharma[1], Basudha Sharma*[2], Indrakant Singh[3], Pratibha Kumari[4]

[1,2]Department of Botany, M.M. College, Modinagar, Ghaziabad, Uttar Pradesh, 201204, India
[3]Department of Zoology, Deshbandhu College, University of Delhi, Kalkaji, New Delhi, 110019, India
[4]Department of Chemistry, Deshbandhu College, University of Delhi, Delhi 110019, India
* Corresponding Author Email:***basudhammc@gmail.com***, +919457981984

Received 22 April 2023, Accepted 22 June 2023, Published 01 August 2023

Abstracts

The application of plant phytometabolites in comparison to other biological approaches for nanoparticle bioreduction has piqued the interest of researchers. This paper reports the phytofabrication of silver nanoparticles. Fresh leaf extracts of *Acokanthera oppositifolia* and *Leucaena leucocephala* were utilized for the reduction and capping of silver ions. The structural properties of nanoparticles were studied using scanning electron microscope (SEM), transmission electron microscopy (TEM), X-ray diffraction (XRD), energy dispersive analysis (EDAX), and Fourier transform infrared spectroscopy (FTIR). The finding reveals that highly crystalline spherical silver nanoparticles produced with an average size of 13.38 nm and 11.93 nm for *Acokanthera oppositifolia* and *Leucaena leucocephala*. The antibacterial activity of synthesized silver nanoparticles was tested against *Bacillus cereus*, *Staphylococcus aureus*, *Enterobacter aerogenes* and *Pseudomonas aeroginosa*. To determine the enhancement in antibacterial activity, the zone of inhibition of the prepared AgNPs was compared to the fresh aqueous extracts, and finding shows that nanoparticles possess more antibacterial activity. So we conclude that Phytomolecule – coated nanoparticles synthesis was found to be a simple, time-saving, cost-effective, and eco-friendly ideal strategy with superior properties.

Keywords: Nanoparticles, Phytomolecule, Capping, Diffractogram, Antibacterial

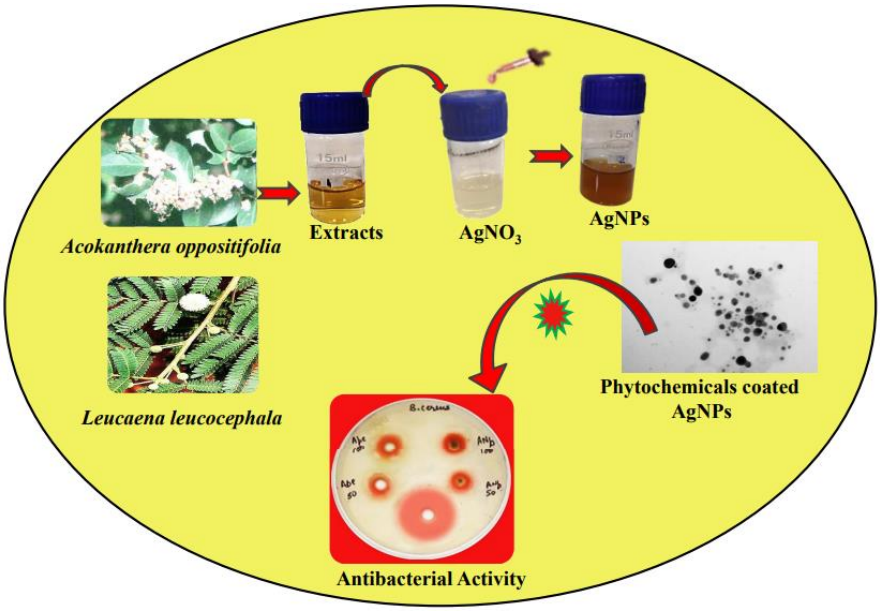

1. Introduction

Nanotechnology beings a technological mammoth at the atomic scale, it had gained more importance in the past few decades. Nanoparticles are the result of manipulating matter at atomic scales from 1 to 100 nm and exhibit improved, novel properties compared to their bulk form. Although nanoparticles are considered a modern scientific invention by Richard Feynman in 1959, they have a very long history since they were used in the 9th century in the Mesopotamian culture for glittering effect on the pot's surface (1). The fact is that Nanoscale particles are the basic foundation of life on earth, as genetic material essential biomolecules for the formation and function of all living cells exist in nano forms. Nanotechnology, according to the National Nanotechnology Initiative (NNI), is the study and engineering of matter at atomic dimensions ranging from 1 to 100 nm that has novel properties that are applicable in various fields (2).

Surface to volume ratio and stronger confinement are the two important factors that play a major role in the change of behavior in nanomaterials. These two principal factors can change or enhance properties such as chemical reactivity, optical activity, strength, and electrical characteristics as compared to their in bulk form (3). Due to these properties, nanoparticles are excessively exploited in different sectors. Various physical, chemical, and biological approaches can be used to fabricate nanoscale particles, among them biological has gained popularity. The problems of physicochemical methods include the use of toxic chemicals, high temperatures, pressures, and the formation of dangerous by-products. However, phytofabrication has gained prominence as a simple method this not only makes the approach environmentally friendly but also more cost-effective. The plant-derived phytochemicals for nanoparticles synthesis has intrigued researchers due to superiority over other biological methods. Unlike microbes, plant extracts does not require complex protocols to maintain sterile microbial cultures and does not exhibit genetic mutations. The plants are widespread, readily available, and affordable. These characteristics make plants a preferred source over microorganisms. Several studies have documented the use of environmentally friendly green approaches to reducing and capping agents in nanoparticle synthesis. Different phytochemicals such as flavonoids, ketones, terpenoids, amides, carboxylicacids, and aldehydes, present in plants are responsible for the reduction, capping, and stabilization of nanoparticles (4).

Metallic nanoparticles such as gold, silver, copper, and zinc are of most interest in the present scenario because of their unique physicochemical properties and superior magnetic, electrical, medical, and optical capabilities. Silver nanoparticles is the most conductible, sensitive, stable, light-absorbing, and has the highest surface plasmon resonance (SPR).Among other nanoparticles, nanosilver is well known for its antibacterial and antioxidant potential. Due to their diverse applications, these are the most commonly used nanoparticles and are exploited in various fields, especially biomedical applications (5).

In recent years, the use of various chemicals and antibiotics has increased rapidly, and antibiotic resistance has become a problem due to the inappropriate use of antibiotics. Addressing this challenge requires a multidisciplinary strategy, including the development of novel antimicrobial agents that have the potential to affect a broad spectrum of microbes. Metal-based nanosilver particles have tremendous potential to combat such kinds of problems for the benevolent of mankind (6). In the Previous findings, metal-based nanoparticles can prevent or overcome biofilm formation, i.e., Gold (7) Silver (8) Magnesium (9) NO, (10), etc. Finding the different literature concludes that, silver nanoparticles can be used in diverse areas safely i.e., in agriculture (11) biomedical (12) cosmetic (13) food packaging (14) textile (15) water purification (16).

In light of these facts, here a study was designed for the phytofabrication and characterization of *Acokanthera oppositifolia* and *Leucaena leucocephala* silver nanoparticles. Further, the difference in antibacterial activity of pure leaves extracts and their prepared nanoparticles also has been investigated.

1.1 Envisaged Reaction Mechanism for Nanoparticles synthesis

There are three major steps in bio-reduction of Ag^{+} to Ag^{0}; reduction and nucleation, aggregation, third capping and stabilization which are represented in (Figure1A). Plant's secondary metabolites play a crucial role like reducing and capping agents (17). *Acokanthera oppositifolia* belongs to the Apocynaceae and is widely used in the traditional medicine system to treat a variety of ailments. In a previously reported study, *Acokanthera oppositifolia* seeds contained palmitate;lup- 20(29)-en-3β-O-(3′-β-hydroxy) triterpene; lupeol, cardiac glycoside; acovenoside A and a sterol; β-sitosterol (18). *Leucaena leucocephala* leaf extracts possess Mimosine, Luteolin-7-o-glucoside, caffeic acid, chrysoeriol, isorhamnetin 3-O-galactoside, kaempferol-3-O-rubinoside, Quercetin-3-O-rhamnoside biomolecules (19, 20, 21, 22). These phytomolecules are assumed to play a key role in reduction and provide stability during nanoparticle fabrication. An envisaged reaction mechanism for the generation of AgNPs represents in (Figure 1B) however, the exact mechanism is still unknown and opens the door for a new research area (23).

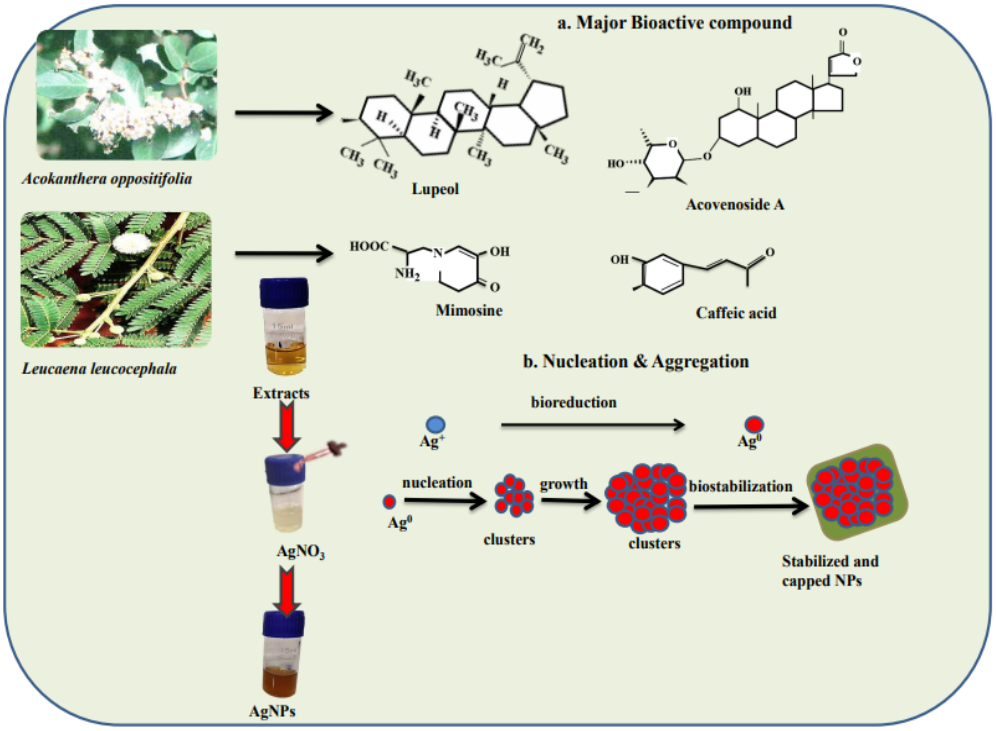

(A)

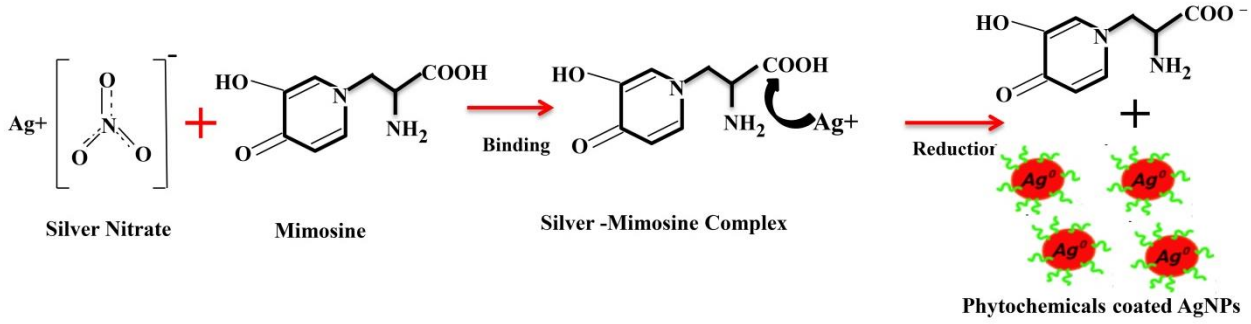

(B)

Figure 1. Schematic representation AgNPs fabrication (A) Various Stages of synthesis (B) Envisaged reaction mechanism for phytofabrication

2. Materials and Methods

2.1 Chemicals

Silver nitrate ($AgNO_3$) salt was purchased from Sigma-Aldrich. Microbial strains of Gram-positive bacteria (*Bacillus cereus*; MTCC430, *Staphylococcus aureus*; MTCC 1144) and Gram-negative bacteria (*Pseudomonas aeruginosa*; MTCC 1864, *Enterobacter aerogenes* MTCC2822) imported from IMTECH Chandigarh were tested for antibacterial potential.

2.2 Preparation of Plant Extracts

Fresh leaves of *Acokanthera oppositifolia* and *Leucaena leucocephala* were collected, taxonomically identified, rinse with tap and distilled water, and air-dried. The dried leaves were coarsely crushed into powder using a grinder. 2g powder dissolved in 100 ml of distilled water and heated at 60°C for one hour. After cooling obtained solution was filtered and stored at 4–8 °C (24).

2.3 Silver nanoparticles phytofabrication

Nanoparticle synthesis was carried out by mixing five milliliters of $AgNO_3$ (25 mM) was mixed with 1 ml of plant extracts (1:5 ratio) to prepare silver nanoparticles, and a color change was observed for up to 24 h. To determine the structural properties of the phytofabricated silver nanoparticles, SEM and TEM micrographs, as well as several spectroscopy techniques, including UV–vis, FTIR, XRD, and EDAX, were used.

2.4 Structural Characterization

To investigate information about the formation, average size, morphology shape, aggregation state, the functional groups involved, and crystalline nature of synthesized nanoparticles a set of characterization techniques were applied (25, 26). The optical properties which confirm the fabrication of nanoparticles were detected as a consequence of the wavelength range of 200 to 800 by using a double beam UV-VIS spectrophotometer (Labtronics Model LT-2201) after optimization. For Sem analysis, Zeiss EVO 18 with acceleration voltage 0.2 to 30 kV was used. For this purpose synthesized aqueous nanoparticles diluted with DW and ultrasonicate, a drop of sample loaded on aluminum stub allowed to dry in stub holder. The morphology and average size of AgNPs were analyzed by transmission electron microscopy (JEOL JEM-1400 maximum accelerating voltage of 120 kV). For transmission electron analysis, ultrasonic dispersion of the synthesized nanoparticles in ethanol and a droplet of this dispersed sample was put onto a carbon-coated copper grid, and dried at room temperature. Energy-dispersive X-ray microanalysis was carried out by using RONTEC's EDX system (Model QuanTax 200) for getting the elemental details. The structural characterization and crystalline nature of powder nanoparticles obtained after centrifugation was analyzed by X-ray profile using X'Pert PRO (PANalytical Netherlands) in the region of 2θ from 30^o to 80^o. The functional groups associated with the production of silver nanoparticles were determined using FTIR analysis. FTIR of dried powder was carried out by Nicolet TM - IS-50 FTIR (Thermo Scientific) through the KBr pellet technique, in the transmission mode range 4000–500 cm-1 through the attenuated total reflectance (ATR) method.

2.5 Comparative Antibacterial potential of phytofabricated AgNPs against their pure extract

2.5.1 Agar well diffusion assay

Antibacterial activity was determined by utilizing an agar well diffusion assay (27). For this purpose, 20 ml of molten NAM was poured into sterile petri dishes and allowed to solidify. Tested microorganisms were swabbed uniformly over the surface of solidified nutrient agar and wells were punched. Prepared well filled with 50 µL and 100 µL of AgNPs and pure plant extracts of both plants. The antibiotic ampicillin (10mg) has been used as a standard. These plates were incubated for 24 hours at 37 °C. The Petri plates were photographed and the

diameter of the inhibition zone was measured through this RIZD % was calculated. Each experiment was performed in triplicate to calculate the mean ± standard deviation by using origin software. The antibacterial activity was calculated using the formula given below (28, 29):

$$Percent\ RIZD\ = \frac{(Nanopartiles\ inhibition\ zone) - \ (Plant\ extracts\ inhibition\ zone)}{(Standard\ inhibition\ zone) - \ (Plant\ exttracts\ inhibition\ zone)} X100$$

2.5.2 Micro-broth dilution method

The minimal inhibitory concentration (MIC) was determined by the micro-broth dilution method. For this, 0.1ml of the cultural broth was inoculated with nanoparticles and pure extracts at concentrations ranging from 1.0 to 50 mg/ml and incubated at 37°C with mixing at 150 rpm in the shaker. After 24 hours, microbial growth was identified by Uv-Visible spectrometric analysis at 600 nm. A broth medium that was free of nanoparticles was used as a positive control. The lowest concentration of nanoparticles that was able to completely inhibit bacterial growth was considered as MIC value (30).

3 Results and Discussion

3.1 AgNPs' UV spectra and visible inspection for color variation

Biosynthesis of AgNPs has been confirmed by color variation, starting light yellowish to orange to finally brown at the primary level and further examined by UV-visible spectroscopy depicted at different time intervals (Figure 2 a, b).After 24 hours further no color change was observed suggesting that the silver salt of the solution was completely reduced. A similar color shift was seen in earlier investigations (31). The color change is due to the strong surface plasmon resonance (SPR) of nanoparticles in an aqueous solution, which is determined by factors like morphological structure, dimension, etc. (32). The UV-Visible spectrum of plant leaf extracts *Acokanthera oppositifolia* and *Leucaena leucocephala* shows a sharp band at 293nm, and 261nm respectively but $AgNO_3$ in aqueous form gives maximum absorbance at 287. Whereas, Uv spectra at 200-600 nm of nanoparticles shifted these absorbance band at 431nm and 436 nm for *Acokanthera oppositifolia* and *Leucaena leucocephala* respectively. After 24 hours, the maximum absorption peak intensity is observed, which indicates complete phytofabrication of silver nanoparticles has taken place in the solution.

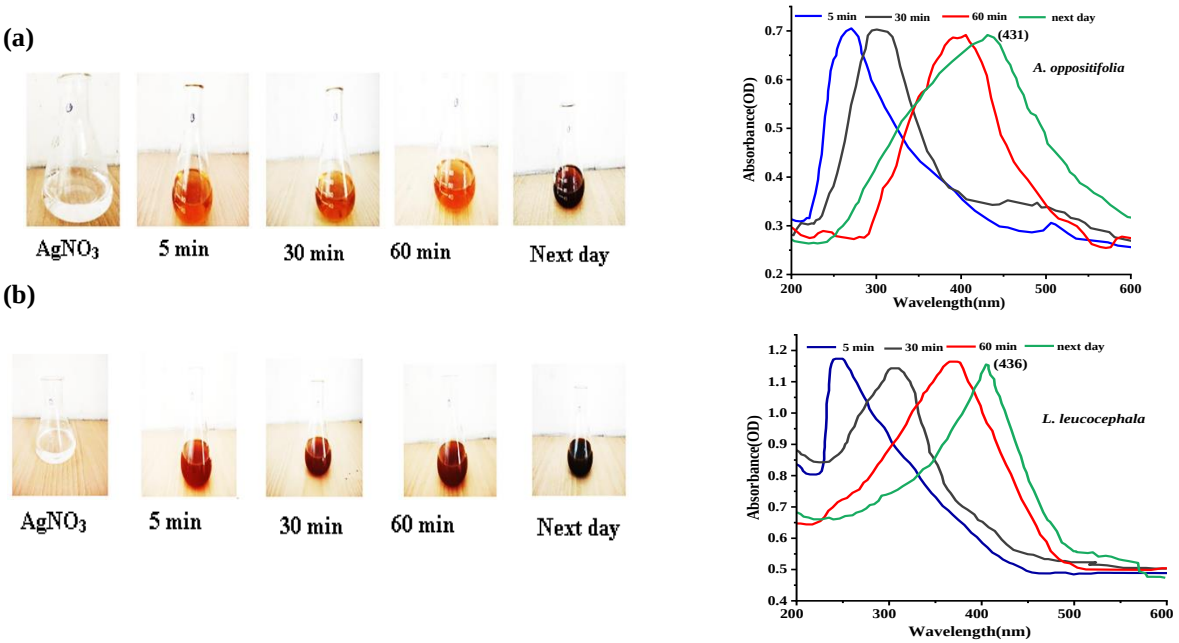

Figure 2. Color variation and Uv-Vis spectrum with time intervals (a) *Aco. oppositifolia* (b) *Leu. leucocephala*

3.2 Structural Characterization

3.2.1 SEM analysis

The shape of the synthesized silver nanoparticles was analyzed by SEM micrograph. Figures 3 and 4 (a) demonstrate that biosynthesized silver nanoparticles are spherical in shape.

3.2.2 TEM analysis

The TEM micrographs of biosynthesized AgNPs are displayed in Figures 3 and 4 (b), which show well-dispersed and spherical-shaped nanoparticles. However, some nanoparticles were observed to be aggregated, but their borders were seen to be lighter than their cores which similar with previous finding of other researcher (33). Some light-colored material found on the surface of nanoparticles indicates phytomolecule capping of the silver nanoparticles, which are responsible for fabrication, these facts are similar to the finding of the previous study by other researchers (33, 34). Particle size distribution of *Acokanthera oppositifolia* AgNPs, was in the ranges of 4 to 27.5 nm with the average size of 11.68 nm ± 0.0273, 11.34 nm ± 0.047, 13.88 nm ± 0.019 at 80,000X 40,000X and 30,000X magnification respectively. Similarly for *Leucaena leucocephala* AgNPs, the ranges from 4.2 to 23.5 nm with the average size of 9.43nm ± 0.028, 14.15nm ± 0.015, 12.68nm ± 0.018 at 80,000X 50,000X and 30,000X respectively shown by histogram. The result of TEM is good agreement crystalline size obtained by XRD. The incorporation of diverse phytomolecules for reduction as well as capping may result in different size distributions of nanoparticles (29). Our findings are comparable to earlier reported 25–50 nm AgNPs produced from *Leucaena leucocephala* seed and leaf extract (19, 35).

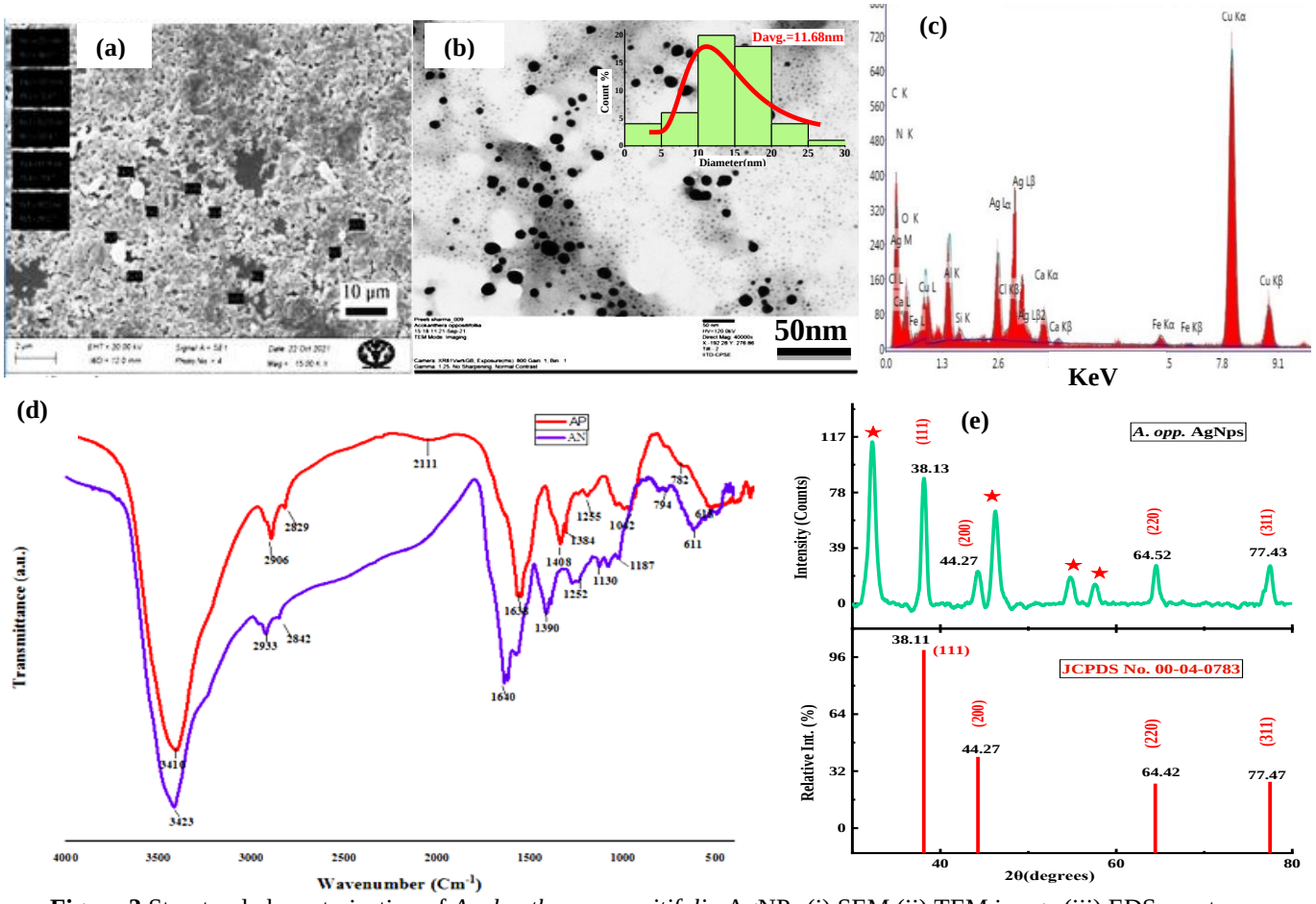

Figure 3.Structural characterization of *Acokanthera oppositifolia* AgNPs (i) SEM (ii) TEM image (iii) EDS spectrum (iv) X- Ray diffractograme (v) FTIR spectrum

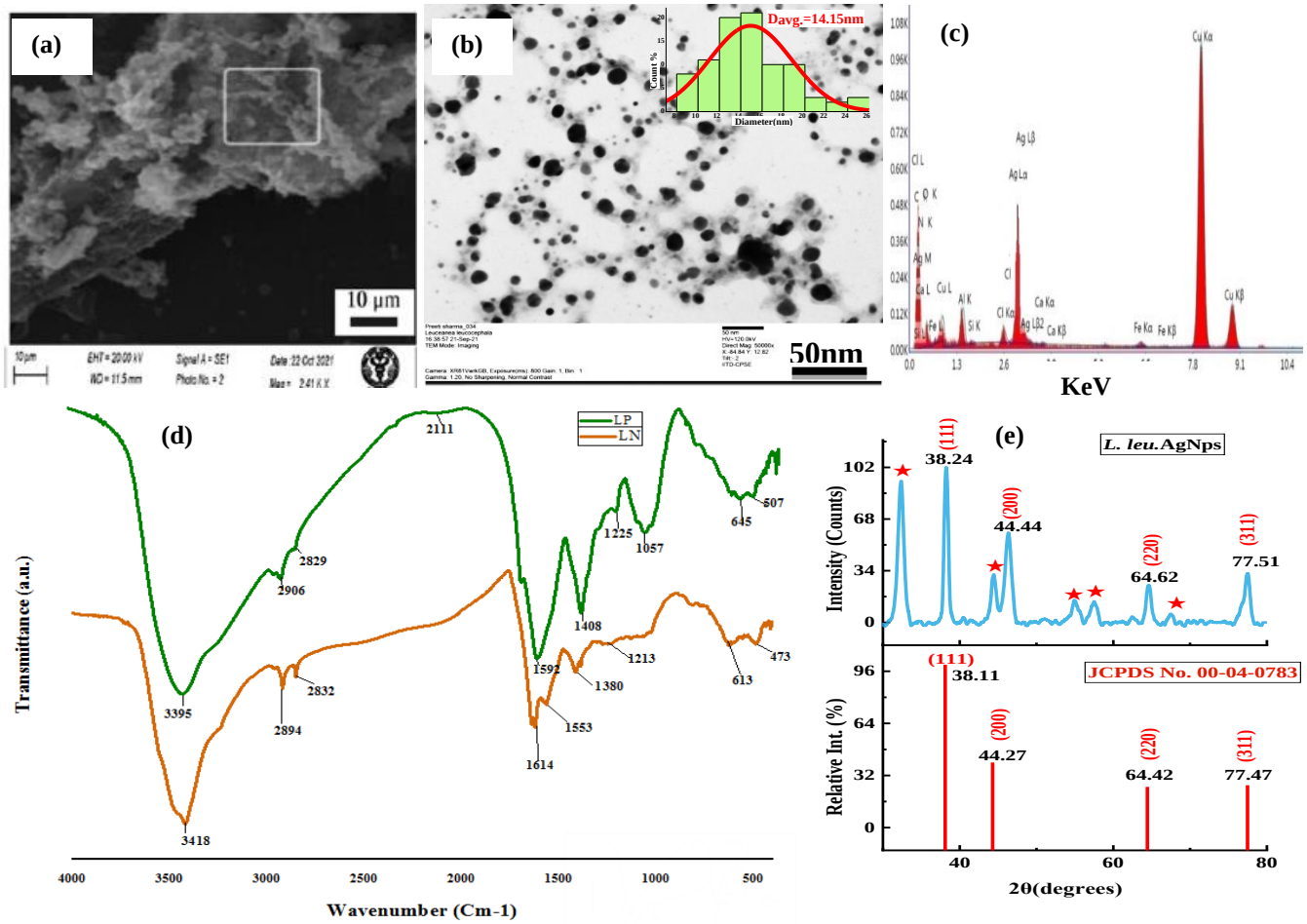

Figure 4. Structural characterization of *Leucaena leucocephala* AgNPs (i) SEM (ii) TEM image (iii) EDS spectrum (iv) X- Ray diffractograme (v) FTIR spectrum

3.2.3 EDAX analysis

The study of the EDX indicates a substantial signal from the silver zone, supporting the silver nanoparticle fabrication represented in Figures 3 and 4 (c). Besides this, the signal for Cu and Al is also present which has come from the TEM grid and holder respectively. Other elements such as chlorine, potassium, carbon, oxygen, calcium, and iron as recorded possibly due to elements from enzymes or proteins (39). The signal for nitrogen might be due to a partial silver nitrate reduction in the reaction mixture or may be present in metabolites of plants.

3.2.4 FTIR scanning

Infrared light scanning, or FTIR, was used to decipher the involvement of phytochemical constituents in the capping and stability of nanoparticles during fabrication. Apart from a few peaks nearby shifting and the emergence of some bands as well, the FTIR spectra of leaf extracts are nearly the same as nanoparticles in both plants, as shown in Figures 3 and 4 (d).This resemblance justifies that some phytochemical constituents of plant extracts hold on to the surface of silver, which is responsible for the reduction as well as stabilization of nanoparticles during the fabrication. Figure 3 (d) represents a strong and wide peak at 3410cm^{-1} characterized by OH stretch of phenolic hydroxyl group presence, 2906 cm^{-1} assigned to C-H stretching of alkane, peak at 2829 cm^{-1} indicates C-H stretching of aldehyde, band at 2111 cm^{-1}assigned to C≡C stretching of Alkyne monosubstituted, 1638 cm^{-1}peakdesignated toalkene C=C stretching, little and sharpen signal at 1408 cm^{-1}characteristics of O-H bending of alcohol, 1255 cm^{-1} position represent (C-N) Stretching of amine, 1042 cm^{-1} indicate CO-O-CO stretching in

anhydride, 782 for C=C bending alkane disubstituted (Cis), a signal at 615 cm^{-1} designated for C-Br halo compound stretching(36, 37, 38). After the reduction and stabilization of silver, the following peaks indicate nearby shifting: 615 to 611, 782 to 794,1042to 1130, 1255 to1252, 1408 to1390, 1638 to 1640,2829 to 2842, 2906 to 2933, 3410 to3423 cm^{-1} indicating that hydroxyl, amide, bromine halo groups may be participating in nanoparticle synthesis. The absence of a 2111 cm^{-1} signal in nanoparticles indicates that alkyne oxidation coupled with silver reduction and increment in signal intensity at 1042 cm^{-1} CO-O-CO stretching in anhydride was also observed.

Figure 4 (d) depicts, that the N-H stretching of aliphatic primary amine can be observed by the strong and broadening peak at 3395 cm^{-1}, C-H stretching of alkanes at 2906 cm^{-1}, and little and sharp band at 1592 cm^{-1}designated for N-H stretching of amide, S=O stretching of sulfonyl chloride represent by a small and sharp peak at 1408 cm^{-1}, C-N stretching of amine at 1225 cm^{-1}, C-O stretching of primary alcohol at 1057, C-Br stretching at 645-507. Whereas after nanoparticle synthesis following peaks indicate nearby shifting from 1225 to 1213, 1408 to 1380, 1592 to1553, 2829 to 2832, 2906 to 2894, 3395 to 3418 to cm^{-1} which indicates that alcohol, bromine halo compound, amide, sulfonyl chloride responsible for silver reduction and stabilization. The absence of 1225 cm^{-1} and 1057 cm^{-1} band in nanoparticle spectra suggests that nitrogen-containing compounds such as mimosine amino acid and alcohol were involved in nanoparticle synthesis. There was also an increase in intensity at 2832 $cm^{-1}$and 2894 cm^{-1}, which represents the involvement of aldehyde and alkane, respectively. A new peak at 1553 cm^{-1} indicates N-O stretching of the nitro compound, and a 1614 cm^{-1}α,β-unsaturated ketone was also detected. The difference in intensity, location and the number of peaks indicate the silver ion reduction.

3.2.5 XRD Profile

The crystallinity of the nanoparticles was determined by comparing the experimental peaks with JCPDS International Center for Data Diffraction File No. 04-0783. They are all indicative of the face-centered cubic structure (fcc), as described in Table 1, by X-ray diffraction profile (40, 41). Different brags reflection peak was obtained for the phytofabricated nanoparticles of *Acokanthera oppositifolia* and *Leucaena leucocephala* which represent in Figures 3 and 4 (e). The calculated d spacing was 2.35, 2.04, 1.44, 1.23Å, for *Acokanthera oppositifolia nanoparticles*, whereas, 2.35, 2.03, 1.44, 1.24, for *Leucaena leucocephala* respectively. As we can see from the the highest peak intensity for (111), among all which depicted maximum amount of nanoparticles growth in this plane and peak sharpening represent particles are in the nano range. Various unassigned peaks may be due to the presence of a capping and stabilizing agent of plant metabolites adsorbed over the surface of nanoparticles. The mean size of the crystal was calculated using the Debye-Scherrer equation D = K/Cos, which represents the X-ray wavelength (1.54), the k Scherer's constant (0.9), the D crystal diameter and the XRD peak FWHM (frequency with half maximum). The average crystalline size reported for *Acokanthera oppositifolia* and *Leucaena leucocephalae* phytofabricated nanoparticles were 13.38 nm and 11.93 nm, respectively as shown in Table2. The outcomes of this analysis also confirmed conformity for SEM and TEM findings.

Table 1. A comparative analysis of the experimental diffraction angle and d-spacing with the standard JCPDS Silver File No. 04-0783 of AgNPs

S.No.	hkl	Reference JCPDS silver:00-04-0783		*Acokanthera opp.* (AgNPs)		*Leucaena leu.* (AgNPs)	
		Standard Diffraction angle (2θ)	d-spacing (Å)	Diffraction angle (2θ)	d-spacing (Å)	Diffraction angle (2θ)	d-spacing (Å)
1.	111	38.11	2.35	38.13	2.35	38.24	2.35
2.	200	44.27	2.04	44.27	2.04	44.44	2.03
3.	220	64.42	1.44	64.52	1.44	64.62	1.44
4.	311	77.47	1.23	77.43	1.23	77.51	1.23

Table 2. Peak Position with D spacing values and average crystallite sizes of *Acokanthera oppositifolia* and *Leucaena leucocephala* AgNPs

	Peak position (2θ)	FWHM degree (β)	d spacing (Å) $d_{hkl}= \lambda/2Sin\ \theta$	Crystalite size D (nm)	D(nm) Average
***Acokanthera oppositifolia* (AgNPs)**	27.816	0.666	3.205	12.282	**13.386**
	32.272	0.775	2.771	10.660	
	38.138	0.531	2.352	15.815	
	44.270	0.634	2.038	13.515	
	46.277	0.703	1.961	12.278	
	54.797	0.737	1.661	12.127	
	57.598	0.650	1.591	13.945	
	64.525	0.598	1.436	15.703	
	77.436	0.719	1.225	14.148	
***Leucaena leucocephala* (AgNPs)**	27.915	0.774	3.193	10.569	**11.936**
	32.345	0.784	2.765	10.548	
	38.249	0.517	2.351	16.255	
	44.440	0.858	2.036	10.000	
	46.322	0.951	1.958	09.080	
	55.042	0.820	1.667	10.921	
	57.474	0.623	1.602	14.522	
	64.620	0.811	1.441	11.588	
	77.511	0.730	1.231	13.937	

3.2 Antimicrobial activity

3.3.1 Zone of inhibition

The antibacterial property of the phytofabricated AgNPs using two different concentrations (50 and 100 µl) of *Acokanthera oppositifolia* and *Leucaena leucocephala*, against four pathogenic bacteria: *Bacillus cereus, Staphylococcus aureus* (Gram-positive), *Enterobacter aerogenes, and Pseudomonas aeroginosa* (Gram-negative) was employed using the agar well diffusion assay. The petri plates in Figure 5 (a-h), showing the inhibition zone. The inhibition zones of nanoparticles and plant extracts are compared to the ampicillin reference. It is observed in Table 3, the antimicrobial efficacy of nanoparticles prepared from leaf extracts of *Acokanthera oppositifolia* is found to be more significant at 13±0.88, 14±0.66, 15±0.88, 16±0.66 mm against *B. cereus, S. aureus, E. aerogenes, P. aeroginosa* bacteria respectively at 100 µl as compare to nanoparticles of *Leucaena leucocephala* at the same concentration. On the other hand, when bacterial strains are treated with pure plant extracts inhibition zone is less as compared to nanoparticles. In contrast, *P. aeroginosa* resists *Acokanthera oppositifolia* pure plant extracts at both the concentration and *B. cereus E. aerogenes* resist by *Leucaena leucocephala* pure plant extracts whereas phytofabricated nanoparticles of these plant extract were found to be effective against these selected microorganisms. Because we detected a larger inhibition zone in the case of bacterial strains treated with nanoparticles, the antibacterial activity of phytofabricated silver nanoparticles is significantly higher than that of their respective pure plant extracts. The nanoparticles exhibited antibacterial efficacy in a dose-dependent manner against all tested microbial cultures because a bigger inhibition zone was observed when using a 100 µl concentration than 50 µl. A similar result was found earlier, in *Leucaena leucocephala* AgNPs where dose-dependent activity was observed and more effective against gram-negative bacteria (19).

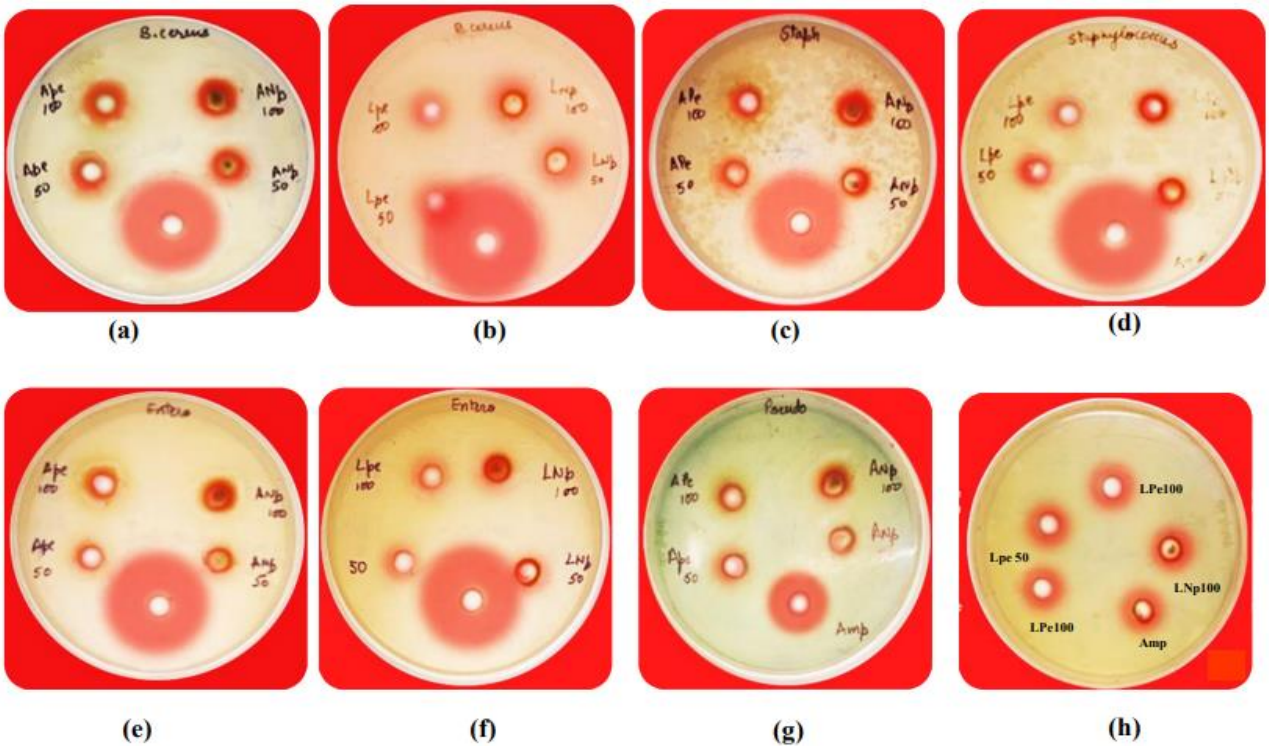

Figure 5. Inhibition zone of pure extracts versus their fabricated AgNPs from *Acokanthera oppositifolia* and *Leucaena leucocephala* respectively; against *Bacillus cereus* (a, b); *Staphylococcus aureus* (c, d); *Enterobacter aerogenes* (e, f); *Pseudomonas aeroginosa* (g, h)

The result in Table 4 indicates that the relative inhibition zone diameter obtained for the gram-negative bacterial strain was more as compared to gram-positive when treated with nanoparticles of these plants. Enhancement in antibacterial activity against gram-negative bacteria may be the result of liberated silver ions by nanoparticles which destroy the cell wall or the result of secondary metabolites adsorbed on the nanoparticle surface, as well as because the cell wall composition is different structurally in gram-positive and gram-negative bacteria (42, 43).

Table 3. Inhibition zone diameter of the aqueous extract of *Acokanthera oppositifolia* and *Leucaena leucocephala* and their AgNPs

		Zone of Inhibition (mm)			
Extracts/ AgNPs	Conc. in µl	*B. cereus*	*S. aureus*	*E. aerogenes*	*P. aeroginosa*
APE	50	9±0.57	8±0.88	9±0.57	-
	100	12±0.57	10±0.57	12±0.88	-
APE-AgNPs	50	10±0.88	10±0.33	9±0.57	10±0.57
	100	13±0.88	14±0.66	15±0.88	16±0.66
LPE	50	-	8±0.57	-	8±0.66
	100	-	9±0.57	10±0.88	10±0.66
LPE-AgNPs	50	8±0.57	10±0.57	11±1.15	10±.57
	100	10±0.88	14±0.88	14±1.45	12±0.57
Ampicillin	10	22±0.12	21±0.0.25	23±0.15	18±0.19

Table 4. Relative Inhibition zone diameter and Minimum inhibition concentration of the aqueous extract of *Acokanthera oppositifolia* and *Leucaena leucocephala* and their AgNPs

Bacterial cultures	RIZD (%)				MIC (mg/ml)			
	ANP50	ANP 100	LNP50	LNP 100	APE	ANP	LPE	LNP
B. cereus	7.60	10.00	36.36	45.45	2.0	1.5	10.0	2.0
S. aureus	15.38	36.36	15.38	41.66	2.0	1.5	2.0	1.5
E. aerogenes	-	27.27	47.82	30.76	1.5	1.5	2.5	1.5
P. aeroginosa	55.55	88.88	20.00	25.00	25.0	1.0	2.0	1.5

3.3.2 MIC values

After 24 h of incubation, no growth of *B. cereus*, *S. aureus*, *E. aerogenes*, *P. aeroginosa*was observed in the test tubes supplemented with 1.5, 1.5, 1.5, 1.0 mg/ml nanoparticles solution of *Acokanthera oppositifolia* which comparable to MIC value 2.0, 1.5, 1.5, 25.0 mg/ml of aqueous extracts of this plant as shown in (Table 4, Figure 6a).The optical density of nanoparticles at 600 nm was found to be 0.40, 0.46, 0.64,and 0.74 against tested pathogenic microorganisms (Figure 6b). Similarly MIC of *Leucaena leucocephala* aqueous extracts was found to be 10.0, 2.0, 2.5, 2.0 mg/ml as compared to their phytofabricated nanoparticles the inhibitory concentration was 2.0, 1.5, 1.5,1.5 mg/ml with optical density 0.40, 0.44, 0.63,0.73 at 600 nm (Figure 6 c). At last, we conclude that antibacterial activity depends on the three-factor Concentration of nanoparticles and type of plant-specific phytochemicals and metabolites in plants, and the type of bacteria due to structural differences. There are supposed to be various mechanisms that make the nanoparticles more susceptible to working as an antibacterial agent. These particles cause damage to bacterial cells by permeating and interfering with DNA, proteins, and other cellular constituents as a consequence of alteration in physical and chemical properties as well as impaired electron transport, permeability, respiration, and osmoregulation (44, 45, 46). Silver nanoparticles liberate silver ions, which act as an antimicrobial according to their dosage and size (47).

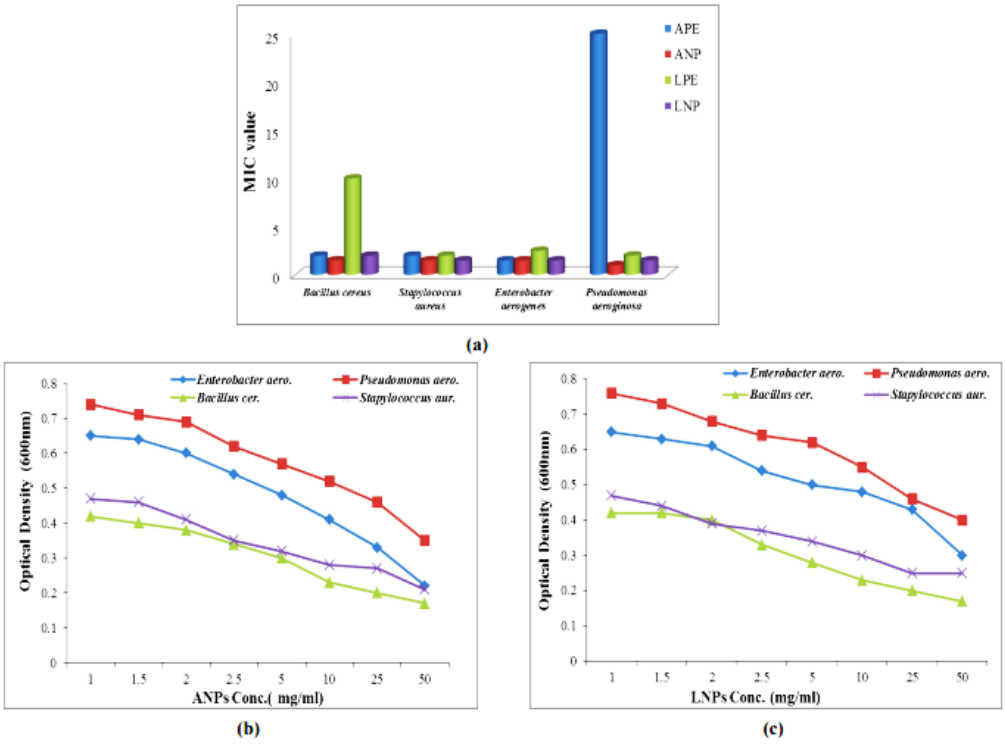

Figure 6. Antimicrobial activity of *Acokanthera oppositifolia* and *Leucaena leucocephala* aqueous extracts and their prepared AgNPs against representative pathogenic microorganisms

4. Conclusions

In this study, effective phytofabrication of spherical-shaped silver nanoparticles of 13.38 and 11.93 nm was achieved using aqueous leaf extracts of *Acokanthera oppositifolia* and *Leucaena leucocephala*, respectively. These nanoparticles possess good antibacterial activity against both gram-positive and gram-negative bacteria compared to their pure aqueous extracts and were found to be more effective against gram-negative bacteria. This may be the consequence of their, size or large surface-to-volume ratio which makes them accessible to readily absorb by cell surface and interact with their intracellular molecules with greater efficiency. Based on the results of the present study, we can conclude that the phytofabrication process is not only a simple, time-saving, cost-effective even environment-friendly and ideal strategy in comparison to other biological chemical and physical methods of nanoparticle synthesis. However, there are still several unsolved questions about how nanoparticles cross the cell membrane and what is the exact antibacterial mechanism? Therefore, this branch is still in its early stages and requires more research, which opens the door to various unanswered problems in this field and paves the way for a broad future scope. Further studies for other prospective applications of these silver nanoparticles are in progress.

5. Acknowledgments

The authors are grateful to the Central Research Facility (CRF) of the Indian Institute of Technology (Delhi) for providing the characterization and AIIMS New Delhi for providing the SEM facility.

6. Conflicts of interest

The authors declare that there are no conflicts of interest.

5. References

1. Feynman RP. There's plenty of room at the bottom [data storage]. Journal of microelectromechanical systems. 1992 Mar;1(1):60-6.
2. NNI (National Nanotechnology Initiative) 2004. What Is Nanotechnology? Available: http://www.nano.gov/html/facts/whatIsNano.html [accessed 16 March 2005].
3. Thangadurai TD, Manjubaashini N, Thomas S, Maria HJ. Fundamentals of nanostructures. InNanostructured Materials 2020 (pp. 29-45). Springer, Cham.
4. Santos CS, Gabriel B, Blanchy M, Menes O, García D, Blanco M, Arconada N, Neto V. Industrial applications of nanoparticles–a prospective overview. Materials Today: Proceedings. 2015 Jan 1;2(1):456-65.
5. Salleh A, Naomi R, Utami ND, Mohammad AW, Mahmoudi E, Mustafa N, Fauzi MB. The potential of silver nanoparticles for antiviral and antibacterial applications: a mechanism of action. Nanomaterials. 2020 Aug;10(8):1566.
6. Wang L, Hu C, Shao L. The antimicrobial activity of nanoparticles: present situation and prospects for the future. International journal of nanomedicine. 2017;12:1227.
7. Yu Q, Li J, Zhang Y, Wang Y, Liu L, Li M. Inhibition of gold nanoparticles (AuNPs) on pathogenic biofilm formation and invasion to host cells. Scientific reports. 2016 May 25;6(1):1-4.
8. Markowska K, GrudniakAM, Wolska KI. Silver nanoparticles as an alternative strategy against bacterial biofilms. ActaBiochimicaPolonica. 2013;60(4).
9. Lellouche J, Friedman A, Lahmi R, Gedanken A, Banin E. Antibiofilm surface functionalization of catheters by magnesium fluoride nanoparticles. International journal of nanomedicine. 2012;7:1175.
10. Hetrick EM, Shin JH, Paul HS, Schoenfisch MH. Anti-biofilm efficacy of nitric oxide-releasing silica nanoparticles. Biomaterials. 2009 May 1;30(14):2782-9.
11. Castillo-Henríquez L, Alfaro-Aguilar K, Ugalde-Álvarez J, Vega-Fernández L, Montes de Oca-Vásquez G, Vega-Baudrit JR. Green synthesis of gold and silver nanoparticles from plant extracts and their possible applications as antimicrobial agents in the agricultural area. Nanomaterials. 2020 Sep;10(9):1763.
12. Zhao P, Deng Y, Xiang G, Liu Y. Nanoparticle-Assisted Sonosensitizers and Their Biomedical Applications. International Journal of Nanomedicine. 2021;16:4615.

13. Domeradzka-Gajda K, Nocuń M, Roszak J, Janasik , Quarles Jr CD, Wąsowicz W, Grobelny J, Tomaszewska E, Celichowski G, Ranoszek-Soliwoda K, Cieślak M. A study on the in vitro percutaneous absorption of silver nanoparticles in combination with aluminum chloride, methyl paraben or di-n-butyl phthalate. Toxicology Letters. 2017 Apr 15;272:38-48.
14. Rezić , Haramina T, Rezić T. Metal nanoparticles and carbon nanotubes—perfect antimicrobial nano-fillers in polymer-based food packaging materials. In Food packaging 2017 Jan 1 (pp. 497-532). Academic Press.
15. Radetić M, Marković D. A review on the role of plasma technology in the nano-finishing of textile materials with metal and metal oxide nanoparticles. Plasma Processes and Polymers. 2022 Apr;19(4):2100197.
16. Hanif Z, Khan ZA, Choi D, La M, Park SJ. One-pot synthesis of silver nanoparticle deposited cellulose nanocrystals with high colloidal stability for bacterial contaminated water purification. Journal of Environmental Chemical Engineering. 2021 Aug 1;9(4):105535.
17. Srikar SK, Giri DD, Pal DB, Mishra PK, Upadhyay SN. Green synthesis of silver nanoparticles: a review. Green and Sustainable Chemistry. 2016 Feb 16;6(1):34-56.
18. El Sayed AM, Ezzat SM, Sabry OM. A new antibacterial lupane ester from the seeds of Acokanthera oppositifolia Lam. Natural product research. 2016 Dec 16;30(24):2813-8.
19. Ghotekar S, Savale A, Pansambal S. Phytofabrication of fluorescent silver nanoparticles from Leucaena leucocephala L. leaves and their biological activities. Journal of Water and Environmental Nanotechnology. 2018 Apr 1;3(2):95-105.
20. Hassan RA, Tawfik WA, Abou-Setta LM. The flavonoid constituents of Leucaena leucocephala growing in Egypt, and their biological activity. African Journal of Traditional, Complementary and Alternative Medicines. 2014;11(1):67-72.
21. Abdelhady NM, Abdallah GM. HPLC/MS/MS study of phenolic compounds of Leucaena leucocephala legumes monitored with their in vitro antihyperglycemic activity. European Journal of Medicinal Plants. 2016:1-9.
22. Chen CY, Wang YD. Steroids from the whole plants of Leucaena leucocephala. American Journal of Analytical Chemistry. 2010 May 1;1(1):31.
23. Kumar B, Smita K, Cumbal L, Debut A, Camacho J, Hernández-Gallegos E, Chavez-Lopez MD, Grijalva M, Angulo Y, Rosero G. Pomosynthesis and biological activity of silver nanoparticles using Passifloratripartita fruit extracts. Advanced Materials Letters. 2015;6(2):127-32.
24. Jain S, Mehata MS. Medicinal plant leaf extract and pure flavonoid mediated green synthesis of silver nanoparticles and their enhanced antibacterial property. Scientific reports. 2017 Nov 20;7(1):1-3.
25. Mourdikoudis S, Pallares RM, Thanh NT. Characterization techniques for nanoparticles: comparison and complementarity upon studying nanoparticle properties. Nanoscale. 2018;10(27):12871-934.
26. Manivasagan P, Venkatesan J, Senthilkumar K, Sivakumar K, Kim SK. Biosynthesis, antimicrobial and cytotoxic effect of silver nanoparticles using a novel Nocardiopsis sp. MBRC-1. BioMed research international. 2013 Jan 1;2013.
27. Nanda A, Saravanan M. Biosynthesis of silver nanoparticles from Staphylococcus aureus and its antimicrobial activity against MRSA and MRSE. Nanomedicine: Nanotechnology, Biology and Medicine. 2009 Dec 1;5(4):452-6.
28. Rojas JJ, Ochoa VJ, Ocampo SA, Muñoz JF. Screening for antimicrobial activity of ten medicinal plants used in Colombian folkloric medicine: A possible alternative in the treatment of non-nosocomial infections. BMC complementary and alternative medicine. 2006 Dec;6(1):1-6.
29. Salayová A, edlovičová , Daneu N, aláž M, Lukáčová ujňáková , alážová Ľ, Tkáčiková Ľ. Green synthesis of silver nanoparticles with antibacterial activity using various medicinal plant extracts: Morphology and antibacterial efficacy. Nanomaterials. 2021 Apr;11(4):1005.
30. Ibrahim HM. Green synthesis and characterization of silver nanoparticles using banana peel extract and their antimicrobial activity against representative microorganisms. Journal of radiation research and applied sciences. 2015 Jul 1;8(3):265-75.

31. Jain S, Mehata MS. Medicinal plant leaf extract and pure flavonoid mediated green synthesis of silver nanoparticles and their enhanced antibacterial property. Scientific reports. 2017 Nov 20;7(1):1-3.
32. Shankar SS, Rai A, Ahmad A, Sastry M. Rapid synthesis of Au, Ag, and bimetallic Au core–Ag shell nanoparticles using Neem (Azadirachtaindica) leaf broth. Journal of colloid and interface science. 2004 Jul 15;275(2):496-502.
33. Das B, Dash SK, Mandal D, Ghosh T, Chattopadhyay S, Tripathy S, Das S, Dey SK, Das D, Roy S. Green synthesized silver nanoparticles destroy multidrug resistant bacteria via reactive oxygen species mediated membrane damage. Arabian Journal of Chemistry. 2017 Sep 1;10(6):862-76.
34. Yasmin A, Ramesh K, Rajeshkumar S. Optimization and stabilization of gold nanoparticles by using herbal plant extract with microwave heating. Nano convergence. 2014 Dec;1(1):1-7.
35. Kumar R, Sharma P, Bamal A, Negi S, Chaudhary S. A safe, efficient and environment friendly biosynthesis of silver nanoparticles using Leucaena leucocephala seed extract and its antioxidant, antimicrobial, antifungal activities and potential in sensing. Green Processing and Synthesis. 2017 Oct 1;6(5):449-59.
36. Coates J. Interpretation of infrared spectra, a practical approach.
37. Kumar JK, Prasad AD. Identification and comparison of biomolecules in medicinal plants of Tephrosiatinctoria and Atylosiaalbicans by using FTIR. Rom. J. Biophys. 2011;21(1):63-71.
38. Kokila T, Ramesh PS, Geetha D. Biosynthesis of AgNPs using Carica Papaya peel extract and evaluation of its antioxidant and antimicrobial activities. Ecotoxicology and Environmental Safety. 2016 Dec 1;134:467-73.
39. Khan M, Karuppiah P, Alkhathlan HZ, Kuniyil M, Khan M, Adil SF, Shaik MR. Green Synthesis of Silver Nanoparticles Using Juniperusprocera Extract: Their Characterization, and Biological Activity. Crystals. 2022 Mar 18;12(3):420.
40. Bykkam S, Ahmadipour M, Narisngam S, Kalagadda VR, Chidurala SC. Extensive studies on X-ray diffraction of green synthesized silver nanoparticles. Adv. Nanopart. 2015 Jan 27;4(1):1-0.
41. Mehta BK, Chhajlani M, Shrivastava BD. Green synthesis of silver nanoparticles and their characterization by XRD. InJournal of physics: conference series 2017 Apr 1 (Vol. 836, No. 1, p. 012050). IOP Publishing.
42. Pazos-Ortiz E, Roque-Ruiz JH, Hinojos-Márquez EA, López-Esparza J, Donohué-Cornejo A, Cuevas-González JC, Espinosa-Cristóbal LF, Reyes-López SY. Dose-dependent antimicrobial activity of silver nanoparticles on polycaprolactone fibers against gram-positive and gram-negative bacteria. Journal of Nanomaterials. 2017 Nov 6;2017.
43. Elemike EE, Onwudiwe DC, Ekennia AC, Katata-Seru L. Biosynthesis, characterization, and antimicrobial effect of silver nanoparticles obtained using Lavandula× intermedia. Research on Chemical Intermediates. 2017 Mar;43(3):1383-94.
44. Nel AE, Mädler L, Velegol D, Xia T, Hoek EM, Somasundaran P, Klaessig F, Castranova V, Thompson M. Understanding biophysicochemical interactions at the nano–bio interface. Nature materials. 2009 Jul;8(7):543-57.
45. Sondi I, Salopek-Sondi B. Silver nanoparticles as antimicrobial agent: a case study on E. coli as a model for Gram-negative bacteria. Journal of colloid and interface science. 2004 Jul 1;275(1):177-82.
46. Su HL, Chou CC, Hung DJ, Lin SH, Pao IC, Lin JH, Huang FL, Dong RX, Lin JJ. The disruption of bacterial membrane integrity through ROS generation induced by nanohybrids of silver and clay. Biomaterials. 2009 Oct 1;30(30):5979-87.
47. Liu J, Sonshine DA, Shervani S, Hurt RH. Controlled release of biologically active silver from nanosilver surfaces. ACS nano. 2010 Nov 23;4(11):6903-13.